PHILOSOPHICAL TRANSACTIONS OF THE ROYAL SOCIETY A MATHEMATICAL, PHYSICAL & ENGINEERING SCIENCES

Magnetoconvection and Thermal Coupling of the Earth's Core and Mantle

Peter Olson and Gary A. Glatzmaier

Phil. Trans. R. Soc. Lond. A 1996 **354**, 1413-1424
doi: 10.1098/rsta.1996.0055

Magnetoconvection and thermal coupling of the Earth's core and mantle

By Peter Olson[1] and Gary A. Glatzmaier[2]

[1]*Department of Earth and Planetary Sciences, Johns Hopkins University, Baltimore, MD 21218, USA*

[2]*Institute of Geophysics and Planetary Physics, Los Alamos National Laboratory, Los Alamos, NM 87515, USA*

Numerical calculations of finite amplitude magnetoconvection in a rotating spherical shell are used to investigate the thermal coupling of the Earth's core to the mantle. From the observed distribution of lower mantle seismic velocity heterogeneity we construct a pattern of heat flow on the core–mantle boundary consisting of a spherical average q_0 plus heterogeneity with amplitude Δq. For $\Delta q/q_0 = 0$, corresponding to a homogeneous lower mantle, convection in the presence of a strong toroidal magnetic field consists of nearly axisymmetric magnetostrophic flow inside the inner-core tangent cylinder and a single large-scale spiraling columnar plume outside the tangent cylinder. Interaction of the columnar plume with the toroidal field induces patches of radial magnetic field distributed symmetrically with respect to the equator. For $\Delta q/q_0 = 10$, corresponding to a strongly heterogeneous lower mantle, stably stratified regions develop below warm mantle and enhanced convection develops below cold mantle. This modulation of the convection pattern breaks the columnar structure of core motions and destroys the equatorial symmetry of the induced magnetic field, without locking it to the mantle. Our results indicate that mantle structure is of secondary importance, compared with rotation, in controlling the structure of the geomagnetic field.

1. Introduction

Convection in the fluid outer core is linked to the structure of the lower mantle in several ways. The average thermal gradient at the base of the mantle determines the total heat flow from the core to the mantle, which in turn governs the cooling rate of the whole core, the rate of inner core solidification and the power available from convection to drive the geodynamo. Convection in the core is also sensitive to lateral variations in lower mantle structure, especially to structure that produces lateral variations in heat flow at the core–mantle boundary (CMB). Variations in radial heat flow at the CMB, resulting from lateral temperature gradients in the lower mantle, produce variations in the radial temperature gradient within the core. This interaction can alter the pattern of convection in the core, enhancing convection where the radial temperature gradients are large and suppressing convection where they are reduced. Because core convection is a major energy source for the geodynamo, modulation of the convection pattern should affect the structure of the geomagnetic field. According to this reasoning, there should exist some relationship between the

Phil. Trans. R. Soc. Lond. A (1996) **354**, 1413–1424
Printed in Great Britain

pattern of mantle heterogeneity as revealed by seismic tomography, the flow in the outer core and the structure of the geomagnetic field. Also, because the pattern of mantle heterogeneity evolves slowly, the coupling with the geomagnetic field should persist for millions of years.

Certain features of the geomagnetic and paleomagnetic field have been cited as examples of this coupling. Much of the present-day geomagnetic field on the CMB is concentrated into four patches with high flux density (Bloxham *et al.* 1989). The patches of flux occur in pairs located symmetrically with respect to the equator, suggesting they may be produced by geostrophic columnar-style convection in the core (Gubbins & Bloxham 1987). The location of the flux patches, and by inference the location of the convection columns, has hardly changed in the past 250 years (Bloxham & Jackson 1992). Models of the paleomagnetic field constructed using directional data from lavas (Constable 1992; Gubbins & Kelly 1993) show patches persisting over the past 2.5 Ma, suggesting they are locked to the mantle. Another feature that has been interpreted as mantle coupling is the apparent concentration of virtual geomagnetic pole paths during polarity reversals. Paleomagnetic data from sedimentary records of recent reversals indicate two preferred trajectories for the virtual pole, one along a longitude passing through the Americas, the other passing through Asia nearly 180° away (Clement 1991; Tric *et al.* 1991). Both of these inferences, locked flux patches and preferred reversal paths, are controversial and the data supporting them has been interpreted in other ways (McFadden *et al.* 1993; Valet *et al.* 1992; Prevot & Camps 1993; Quidelleur *et al.* 1994). Indeed, the controversies surrounding these interpretations highlight the need for a more complete theoretical investigation of the phenomenon.

In order to theoretically determine which properties of the core convection and the geomagnetic field are most sensitive to the thermal structure of the mantle, it is first necessary to understand the dynamics of convection in the core subject to homogeneous boundary conditions, and then determine how the picture changes when the heterogeneity imposed by the mantle is included. There have been several efforts to model this interaction using numerical calculations of thermal convection in a rotating spherical shell driven by temperature heterogeneity on the outer boundary (Zhang & Gubbins 1993; Sun *et al.* 1994). The Zhang & Gubbins (1993) study was restricted to small amplitude convection (very near the critical Rayleigh number for the onset of motion) and relatively low rotation rates. Their calculations exhibited a mixed response, consisting of a baroclinic flow locked to the mantle temperature structure and a propagating convection pattern. The Sun *et al.* (1994) study examined convection at a Rayleigh number five times critical and higher rotation rates. They reported a form of coupling in which the pattern of flow was locked to the pattern of thermal heterogeneity on the boundary. Importantly, neither of these studies included the Lorentz force due to the magnetic field, which is known to strongly influence the structure of convection in rotating electrically conducting fluids and is a dominant force in the Earth's core (Fearn *et al.* 1994; Zhang & Jones 1994; Zhang 1995; Olson & Glatzmaier 1995; Cardin & Olson 1995). The pattern of convection in a rotating sphere changes so drastically when the Lorentz force is added that it is dangerous to interpret core–mantle thermal interaction using models of non-magnetic convection.

In this paper we present numerical calculations of finite amplitude thermal convection in a rotating electrically conducting self-gravitating fluid with an imposed azimuthal magnetic field. We compare two calculations, one with homogeneous tem-

Table 1. *Dimensionless parameters*

parameter	definition	outer core	calculation 1	calculation 2
Pm	ν/λ	10^{-4}–10^{-5}	10^{-2}	10^{-2}
Pr	ν/κ	0.1–10	1	1
E	$\nu/(2\Omega D^2)$	$\simeq 10^{-12}$	5×10^{-5}	5×10^{-4}
Ra	$\alpha g_o \Delta T D^3/(\kappa\nu)$	$\simeq 10^{20}$	1×10^{7}	$\simeq 1\times10^{7}$
Λ	$\sigma B^2/(2\Omega\rho)$	0.1–10	10	10
$\Delta q/q_0$	$(q_{\max}-q_0)/q_0$	0–10	0	10
R	r_i/r_o	0.35	0.35	0.35

perature on the outer boundary and the other with heterogeneous heat flow boundary conditions derived from the seismic structure of the lower mantle.

2. Magnetoconvection in a rotating spherical shell

Consider the motion of a self-gravitating Boussinesq fluid in a spherical coordinate system (r,θ,ϕ) rotating with uniform angular velocity $\Omega\hat{\boldsymbol{z}}$. The fluid is electrically conducting and subject to buoyancy forces produced by temperature variations and to Lorentz forces produced by interaction between electrical currents and magnetic fields. In dimensionless form the equations of motion are

$$E\left(\frac{\partial \boldsymbol{u}}{\partial t}+\boldsymbol{u}\cdot\nabla\boldsymbol{u}-\nabla^2\boldsymbol{u}\right)+\hat{\boldsymbol{z}}\times\boldsymbol{u}+\nabla P = Pr^{-1}\,E\,Ra\,\boldsymbol{r}T+Pm^{-1}\,\Lambda(\nabla\times\boldsymbol{B})\times\boldsymbol{B}, \tag{2.1}$$

$$\nabla\cdot(\boldsymbol{u},\boldsymbol{B})=0, \tag{2.2}$$

$$\frac{\partial T}{\partial t}+\boldsymbol{u}\cdot\nabla T = Pr^{-1}\,\nabla^2 T, \tag{2.3}$$

$$\frac{\partial \boldsymbol{B}}{\partial t}=\nabla\times(\boldsymbol{u}\times\boldsymbol{B})+Pm^{-1}\,\nabla^2\boldsymbol{B}, \tag{2.4}$$

where $\boldsymbol{B}$, $\boldsymbol{u}$, P and T are magnetic induction, velocity, pressure and temperature perturbations, respectively. The dimensionless parameters are the Ekman number $E=\nu/(2\Omega D^2)$, the Prandtl number $Pr=\nu/\kappa$, the magnetic Prandtl number $Pm=\nu/\lambda$, the Rayleigh number $Ra=\alpha g_o\Delta T D^3/(\kappa\nu)$ and Elsasser number $\Lambda=\sigma B^2/(2\Omega\rho)$. Here D is the spherical shell thickness, ν is kinematic viscosity, κ is thermal diffusivity, λ is magnetic diffusivity, α is thermal expansivity, g_o is gravity at the outer spherical boundary, ρ is the fluid density, σ is electrical conductivity and ΔT is the temperature difference between the inner and outer spherical boundaries. Table 1 gives values of the dimensionless parameters used in the calculations as well as order-of-magnitude estimates for the core.

Calculations are made using the following boundary conditions. The inner and outer boundaries of the spherical shell are treated as solid surfaces so that

$$\boldsymbol{u}=0,\quad r=r_i,\quad r=r_o. \tag{2.5}$$

In addition, the mantle and inner core are assumed to be electrically non-conducting,

so the radial component of the current density vanishes at both boundaries:

$$J_r = 0, \quad r = r_\mathrm{i}, \quad r = r_\mathrm{o}, \tag{2.6}$$

which requires the toroidal part of the magnetic field to vanish and the poloidal part of the magnetic field to match an exterior potential field at $r = r_\mathrm{o}$ and an interior potential field at $r = r_\mathrm{i}$.

Magnetoconvection in the fluid shell is maintained by prescribing a non-homogeneous boundary condition for the toroidal field at the inner boundary and the appropriate thermal boundary conditions. An axisymmetric toroidal magnetic field is maintained in the shell by setting

$$B_\phi = \sin(2\theta), \quad r = r_\mathrm{i}. \tag{2.7}$$

Note that this condition imposes oppositely directed maxima in the toroidal field at $\theta = \frac{1}{2}\pi \pm \frac{1}{4}\pi$. The Elsasser number is defined in terms of these field intensities. In addition, the temperature is fixed on the inner boundary, so that

$$T = 1, \quad r = r_\mathrm{i}. \tag{2.8}$$

Two different thermal conditions are used at the outer boundary. The first calculation uses an isothermal condition

$$T = 0, \quad r = r_\mathrm{o}. \tag{2.9}$$

In the second calculation, the heat flux is fixed. We express the outer boundary heat flux as the sum of a spherical average plus a deviation

$$q = q_\mathrm{o} + \delta q(\theta, \phi), \quad r = r_\mathrm{o}. \tag{2.10}$$

The spherical average term q_o is set equal to the spherically and temporally averaged heat flow from the fixed temperature calculation. The deviation $\delta q(\theta, \phi)$ is given by

$$\delta q = C \delta V_\mathrm{s}, \tag{2.11}$$

where $\delta V_\mathrm{s}(\theta, \phi)$ is the Su *et al.* (1994) model of lower mantle seismic heterogeneity (including only spherical harmonics up to degree 4) and C is a scale factor. We adjust the factor C such that Δq, the maximum heat flow variation relative to q_0, the mean on the CMB, is ten times q_0. This variation is typical of models of thermal convection in the lower mantle (Bercovici *et al.* 1989; Tackley *et al.* 1994). It produces a heterogeneous temperature distribution on the CMB, with low temperatures occurring where heat flows from the core to the mantle, and high temperatures where the heat flow is from the mantle to the core, as shown in figure 2.

The numerical model was developed for rotating convection by Glatzmaier & Olson (1993) and extended to rotating magnetoconvection by Olson & Glatzmaier (1995). A closely related version of the model is currently being applied to the full dynamo problem (Glatzmaier & Roberts 1995) The three components of velocity, three components of magnetic field, the pressure and the temperature are updated every timestep by solving equations (2.1)–(2.4). All variables are expanded in spherical harmonics to resolve their horizontal structures and in Chebyshev polynomials to resolve their radial structures. A spectral transform method is used to compute nonlinear terms. The second-order time integration treats the linear terms implicitly and the nonlinear terms explicitly. The calculations presented here used all spherical harmonic degrees and orders up to 106 and Chebyshev polynomials up to degree 48. Starting from a conductive state with small random perturbations, the solution

PHILOSOPHICAL TRANSACTIONS OF THE ROYAL SOCIETY A MATHEMATICAL, PHYSICAL & ENGINEERING SCIENCES

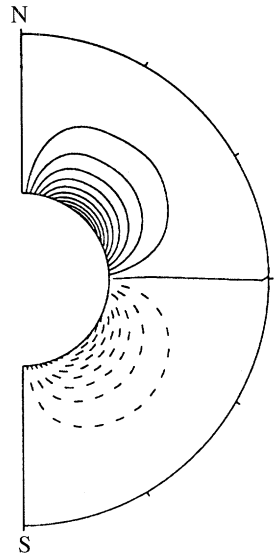

Figure 1. Contours of the initial axisymmetric toroidal magnetic field. Solid and dash contours indicate eastward and westward directed field, respectively.

was integrated forward in time until the change in total kinetic and magnetic energy became negligibly small. Although these flows are inherently time dependent, they appear to reach a statistically equilibrated state characterized by a persistent structure.

3. Results

Figures 1–5 compare the results of the two calculations, for the parameter values listed in table 1. The figures show the flow structure after approximately 100 000 time steps (approximately 20 magnetic diffusion times), in the fully developed regime.

Figure 1 shows contours of the initial toroidal magnetic field, the zero-velocity steady-state solution to (2.4) with boundary conditions (2.6), (2.7). The toroidal field is concentrated in two azimuthal bundles, one in each hemisphere, with opposing polarity. The Elsasser number $\Lambda = 10$ corresponds to a maximum toroidal field intensity of about 5–10 mT in the core. Two calculations are compared in figures 3–5, the homogeneous case with an isothermal outer boundary and the heterogeneous case with variable heat flow on the outer boundary.

Before contrasting the flows produced in these two calculations, it is useful to describe the effect of heterogeneous heat flow on temperatures at the outer boundary. Figure 2 shows the boundary heat flow variation $\delta q(\theta, \phi)$ and the resulting boundary temperature variation. Both the heat flow and the boundary temperature variation exhibit the spherical-harmonic degree-two pattern that dominates the seismic velocity structure in the lower mantle. The heat flow and temperature are negatively correlated. Low boundary temperatures occur in regions where heat flows from the core to the mantle and high boundary temperatures occur where heat flows in the opposite direction, from the mantle to the core. The difference in the shape of isotherms in the low- and high-temperature regions on the boundary is significant in the core. High-temperature regions have smooth isotherms, indicating conductive

PHILOSOPHICAL TRANSACTIONS OF THE ROYAL SOCIETY A MATHEMATICAL, PHYSICAL & ENGINEERING SCIENCES

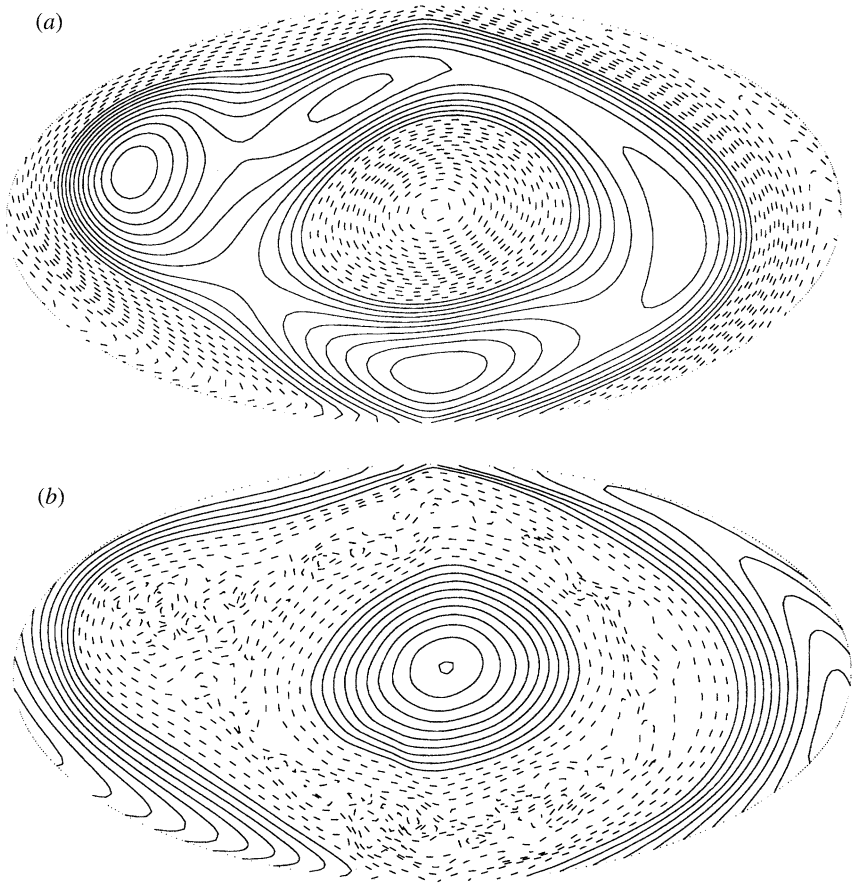

Figure 2. (*a*) Variations in radial heat flow (relative to the mean) applied to outer boundary in the heterogeneous heat flow calculation, derived from lower mantle seismic tomography model of Su *et al.* (1994) truncated at spherical harmonic degree and order 4. (*b*) Outer boundary temperature variations resulting from heat flow variations. Solid and dash contours indicate positive and negative values, respectively.

heat transfer, whereas the low-temperature regions have irregular isotherms, indicative of convective heat transfer. The calculations demonstrate that a major effect of heterogeneous boundary heat flow is to alter the pattern of core convection. Where the CMB temperature is low and heat flows from the core to the mantle, the local thermal stratification is superadiabatic and convection is vigorous. Where the CMB temperature is high and heat flows from the mantle to the core, the local thermal stratification is subadiabatic and convection is reduced or suppressed.

Figure 3 shows snapshots of the motion and temperature in axial and equatorial sections from the two calculations. In the homogeneous case, the style of convection is controlled by the *tangent cylinder*, an imaginary cylinder circumscribing the inner core and concentric with the rotation axis. The flow is most vigorous inside the tangent cylinder, and as the images in figure 4 indicate, consists of nearly axisymmetric convection. Outside the tangent cylinder the flow is weaker and is organized along columns displaced from, but parallel to, the rotation axis. Columnar flow is the preferred mode of convection in this region, even in the presence of a strong mag-

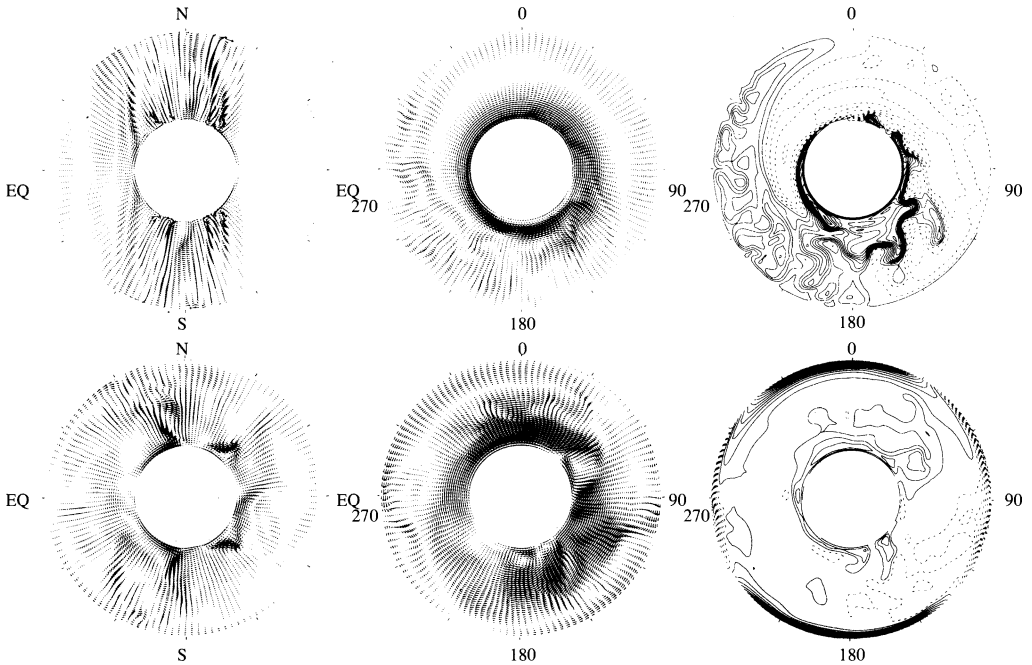

Figure 3. Great circle snapshots of magnetoconvection in a rotating spherical shell. Top row shows convection driven by uniform temperature boundary condition. Bottom row shows convection driven by heterogeneous heat flow boundary condition. Left column, velocity vectors in an axial plane; middle column, velocity vectors in the equatorial plane, viewed toward the north; right column, temperature perturbation contours in the equatorial plane, viewed toward the north. Solid and dash contours indicate positive and negative values, respectively.

netic field (Zhang 1995; Olson & Glatzmaier 1995). The planform of the columns in the equatorial plane depends on the magnetic field strength through the Elsasser number. An equatorial planform consisting of small diameter columns is preferred when the Elsasser number is small, whereas the equatorial planform consists of large diameter spiral-shaped columns when the Elsasser number is of order one or greater (Cardin & Olson 1995; Olson & Glatzmaier 1995). In the homogeneous case, the equatorial planforms shown in figure 3 contain a single large-scale spiral-shaped rising plume, with many smaller-scale instabilities imbedded within it. The motion generated by the spiral plume is predominantly azimuthal, that is, nearly parallel to the toroidal magnetic field lines. Spiral-shaped convection columns are preferred because they satisfy approximately both the constraints of rotation (vorticity aligned with rotation) and of the Lorentz force (flow parallel to magnetic field).

Figure 4 shows the pattern of temperature variations, radial velocity and radial magnetic field near the outer boundary. The large spiral plume is evident in the temperature field at low latitudes, and the pattern of radial velocity indicates this plume drives a geostrophic flow in the region outside the tangent cylinder comprised of columnar upwellings and downwellings with a high degree of symmetry across the equator. The images in figure 4 show that the motion inside the tangent cylinder is generally more vigorous than outside, and is quite different in character. Instead of geostrophic columns, the motion above and below the inner core is more axisymmetric and consists of a series of concentric rings of rising and sinking fluid with several concentrated small-scale upwelling spots. This convection is more nearly

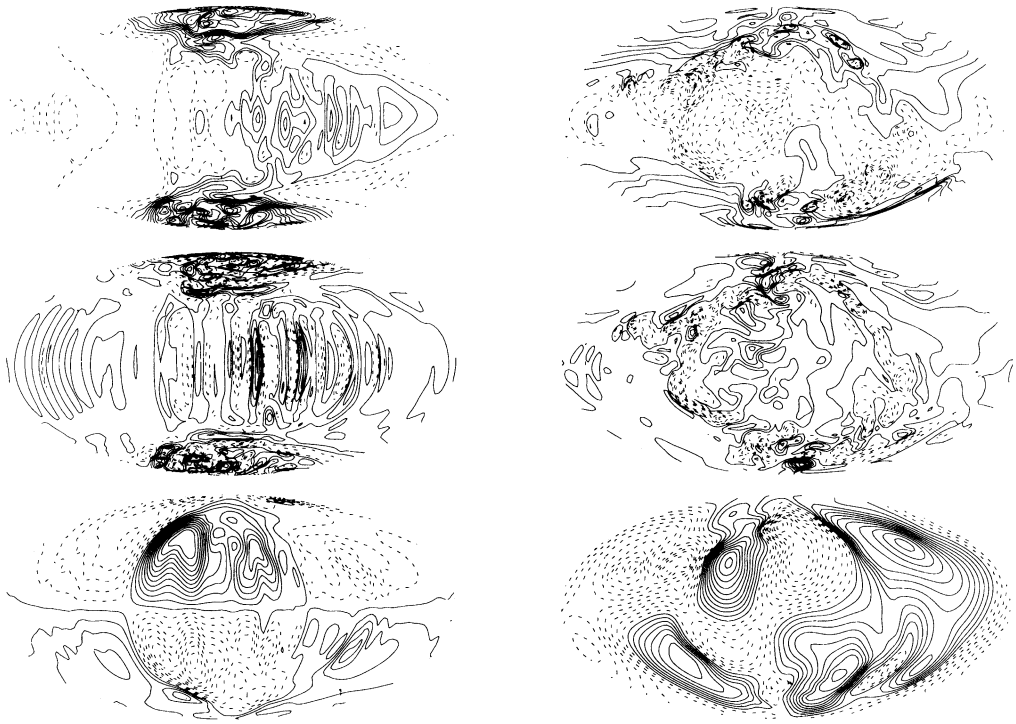

Figure 4. Orthographic snapshots of magnetoconvection in a rotating spherical shell. Left column shows convection driven by uniform temperature boundary conditions. Right column shows convection driven by heterogeneous heat flow boundary condition. First row, temperature perturbations at $r/r_o = 0.84$; second row, radial velocity at $r/r_o = 0.84$; third row, radial magnetic field at $r/r_o = 1.0$. Solid and dash contours indicate positive and negative values, respectively.

magnetostrophic, in that it transports heat without bending the toroidal magnetic field lines and thereby avoids large Lorentz forces.

The magnetic field at the outer boundary is almost entirely induced by the geostrophic part of the flow. As shown on the left in figure 4, the induced magnetic field consists of patches of concentrated flux arrayed symmetrically with respect to the equator. As other studies have demonstrated, these patches form where upwelling columns of fluid bend the toroidal field into loops (Cardin & Olson 1995). The two intense patches in the homogeneous case shown in figure 4 are located just upstream of the spiral plume. The flux patches are attached to the major upwellings and precess around the sphere in the prograde sense. Note that the convection within the tangent cylinder induces very little magnetic field, consistent with its magnetostrophic character.

The structure of the axisymmetric part of the induced magnetic field and the variations in angular velocity associated with the flow are shown in figure 5. In the homogeneous case the axisymmetric part of the field is dominated by the pair of intense flux patches and is approximately octopolar. The variations in angular velocity (relative to the fixed rotation of the solid boundaries) are geostrophic outside the tangent cylinder. The direction of motion associated with the angular velocity distribution changes from prograde near the tangent cylinder to retrograde near the equator. Both above and below the inner core, the presence of radial shear in the angular velocity indicates the zonal flow inside the tangent cylinder consists of

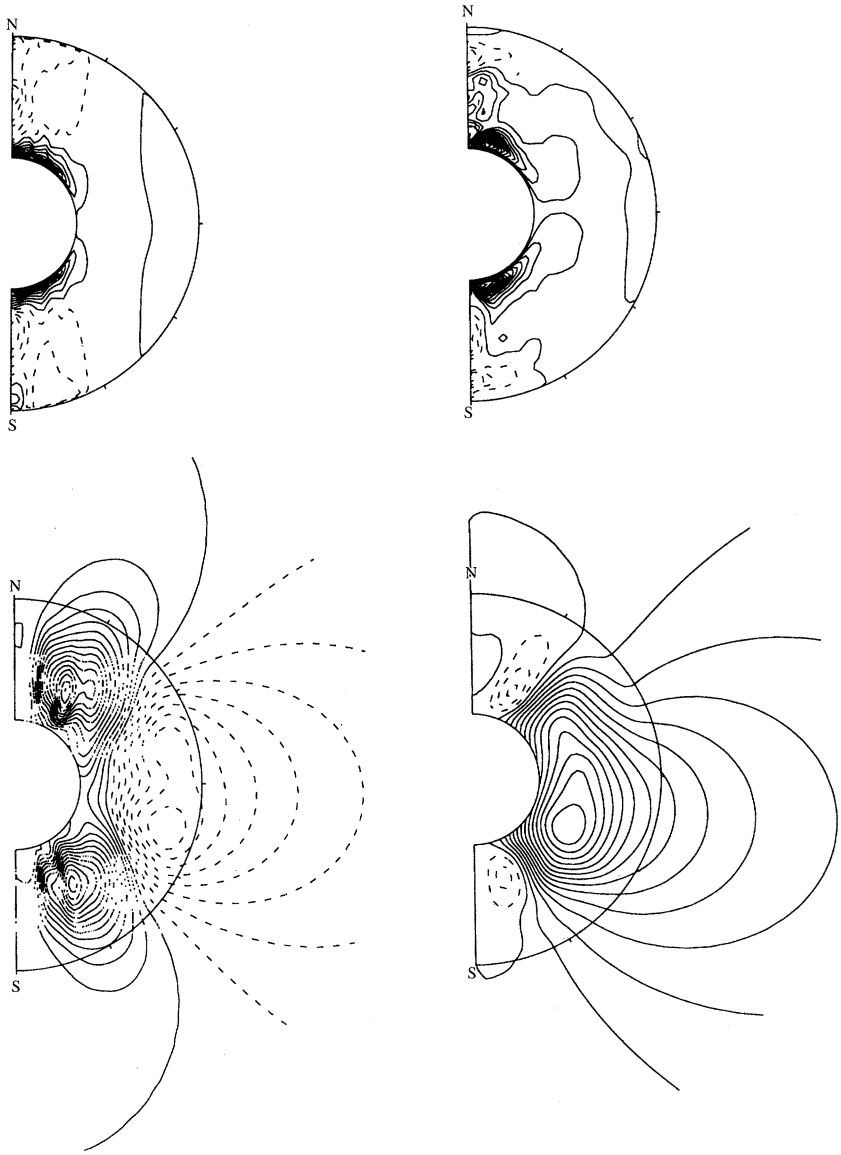

Figure 5. Longitudinally averaged structure of magnetoconvection in a rotating spherical shell. Left column shows convection driven by uniform temperature boundary conditions. Right column shows convection driven by heterogeneous heat flow boundary condition. First row, angular velocity variations relative to angular velocity of solid boundaries; solid and dash contours indicate prograde and retrograde (relative) angular motion, respectively. Second row, lines of force of longitudinally averaged poloidal magnetic field. Solid and dash curves indicate clockwise and counterclockwise directed field lines, respectively.

strong thermal wind. Accordingly, the angular velocity of the fluid near the inner boundary is larger than that near the outer boundary. This effect could be further accentuated had we not fixed the angular velocity of the inner core, but allowed it to be determined dynamically.

Heterogeneous heat flow at the outer boundary imposes a pattern of lateral temper-

PHILOSOPHICAL TRANSACTIONS OF THE ROYAL SOCIETY A MATHEMATICAL, PHYSICAL & ENGINEERING SCIENCES

ature gradient that alters the structure of the convection and the induced magnetic field. The great circle sections in figure 3 demonstrate that circulation driven by the lateral thermal gradients overwhelms both the geostrophic convection columns in the region outside the tangent cylinder and the magnetostrophic convection inside the tangent cylinder. The motion near the outer boundary consists of a ring of surface convergence and convective downwelling beneath the regions where the heat flow is from the core to the mantle, plus broad surface divergence and weak upwellings beneath the regions where the heat flow is from the mantle to the core. Plumes originating at the inner boundary are disrupted by this circulation and consequently do not appear in the images in figure 4. The induced magnetic field at the outer boundary consists of sectors of radial flux spanning the equator, rather than patches of flux symmetric about the equator. This pattern nonetheless propagates around the sphere with a time-dependent (non-steady) phase speed, indicating it is generated by the interior convection rather than the circulation locked to the boundary heterogeneity. Accordingly, the role played by the boundary heterogeneity is not to create a component of the field tied to the mantle structure. Instead, it drives an incompatible circulation which breaks the natural structure of the convection and destroys the equatorial symmetry of the induced magnetic field.

4. Discussion

The thermal coupling we describe in this paper has little effect on the mantle. The temperature variations on the CMB produced by this interaction are far too small to influence convection in the lower mantle. When scaled to core conditions, the CMB temperature variations produced in our calculation using heterogeneous boundary heat flow amount to less than 1 K. Accordingly, it is reasonable to assume the mantle responds to the core as if it were an isothermal reservoir, to a very good approximation.

In contrast, heat flow variations on the CMB are very significant for core dynamics, for two reasons. First, the low viscosity core fluid is extremely sensitive to lateral thermal gradients. The second reason is more subtle, and involves the role of the adiabat in core dynamics. The convective energy budget of the core is limited by the total rate of heat transfer to the mantle. Estimates of the heat transfer from the core to the mantle, ranging from 2 TW up to perhaps 10 TW, are hardly larger than, and in fact are comparable to, the heat conducted down the adiabatic gradient in the core (Buffett *et al.* 1992). Traditionally, the near equality between total heat loss and adiabatic conduction has been interpreted to mean thermal convection in the core is marginal or even suppressed (Loper 1990).

Our calculations offer a new interpretation. Because heat flow varies over the CMB, thermal convection is *inevitably* a significant part of core motions. The convection originates in the regions below the CMB where the heat flow is from the core to the mantle. The fraction of the CMB that supports convection corresponds to the fraction of the surface area where the *local* heat flow exceeds the heat conducted down the adiabat. In our calculations with heterogeneous CMB heat flow, thermal convection in the outer part of the core occurs beneath the circum-Pacific ring of high seismic velocities in the lower mantle, and does not have the columnar structure found in the calculation with homogeneous boundary conditions. Beneath the other portions of the CMB, the model heat flow is inward, from the mantle to the core, and convection is suppressed in these regions. Deeper within the shell, the convection is

PHILOSOPHICAL TRANSACTIONS OF THE ROYAL SOCIETY A MATHEMATICAL, PHYSICAL & ENGINEERING SCIENCES

less dominated by effects of the outer boundary, and is more controlled by Lorentz and Coriolis forces. Accordingly, this portion of the flow drifts from west to east and is not locked to the mantle.

Because only the outermost portion of the fluid shell couples to the boundary heterogeneity in our calculations, the induced magnetic field is not locked to mantle structure. Instead of fixing the position of the geostrophic convection columns, we find that the boundary heterogeneity tends to break the columnar structure, by imposing secondary flows that extend some distance below the outer boundary. Since the convection is not columnar, the induced magnetic field is not symmetric about the equator. Nonetheless, the convection pattern retains its azimuthal drift, causing the magnetic field to propagate along with the convection.

On the basis of these calculations, convection with large boundary heterogeneity may actually be a less satisfactory model of the core than convection with homogeneous boundary conditions. We know that the magnetic field is highly symmetric in a time-average sense (Merrill & McElhinny 1983; Constable 1992; Quidelleur *et al.* 1994), and the flow near the CMB has a degree of equatorial symmetry as well (Hulot *et al.* 1990; Voorhies 1993). Of course, these calculations are not close enough to core conditions to draw specific conclusions, but they do make general predictions that are testable. We find that equatorial symmetry and columnar structure are properties of core convection free of mantle heterogeneity, and the resulting magnetic field is concentrated in symmetric patches. The primary effects of mantle heterogeneity are to destroy the symmetry and columnar structure of core convection and break the equatorial symmetry of the magnetic field.

References

Bercovici, D., Schubert, G. & Glatzmaier, G. A. 1989 Influence of heating mode on three-dimensional mantle convection. *Geophys. Res. Lett.* **16**, 617–620.

Bloxham, J. & Jackson, A. 1992 Time-dependent mapping of the geomagnetic field at the core–mantle boundary. *J. Geophys. Res.* **97**, 19 357-19 564.

Bloxham, J., Gubbins, D. & Jackson, A. 1989 Geomagnetic secular variation. *Phil. Trans. R. Soc. Lond.* A **329**, 415–502.

Buffett, B. A., Huppert, H. E., Lister, J. R. & Woods, A. W. 1992 Analytical model for solidification of the Earth's core. *Nature* **356**, 329–331.

Cardin, P. & Olson, P. 1992 An experimental approach to thermochemical convection in the Earth's core. *Geophys. Res. Lett.* **19**, 1995–1998.

Cardin, P. & Olson, P. 1994 Chaotic thermal convection in a rapidly rotating spherical shell: consequences for flow in the outer core. *Phys. Earth Planet. Inter.* **82**, 235–259.

Clement, B. M. 1991 Geographical distribution of transitional VGPs: evidence for non-zonal equatorial symmetry during the Matuyama–Brunhes geomagnetic reversal. *Earth Planet. Sci. Lett.* **104**, 48–58.

Constable, C. G. 1992 Link between geomagnetic reversal paths and secular variation of the field over the past 5 Ma. *Nature* **358**, 230–233.

Fearn, D. R. 1979 Thermally driven hydromagnetic convection in a rapidly rotating sphere. *Proc. R. Soc. Lond.* A **369**, 227–242.

Fearn, D. R., Proctor, M. R. E. & Sellar, C. C. 1994 Nonlinear magnetoconvection in a rapidly rotating sphere and Taylor's constraint. *Geophys. Astrophys. Fluid Dyn.* **77**, 111–132.

Glatzmaier, G. A. & Olson, P. 1993 Highly supercritical thermal convection in a rotating spherical shell: centrifugal vs. radial gravity. *Geophys. Astrophys. Fluid Dyn.* **70**, 113–136.

Glatzmaier, G. A. & Roberts, P. H. 1995 A three-dimensional convective dynamo solution with rotating and finitely conducting inner core and mantle. *Phys. Earth Planet. Inter.* **91**, 63–75.

PHILOSOPHICAL TRANSACTIONS OF THE ROYAL SOCIETY A MATHEMATICAL, PHYSICAL & ENGINEERING SCIENCES

Gubbins, D. & Bloxham, J. 1987 Morphology of the geomagnetic field and implications for the geodynamo. *Nature* **325**, 509–511.

Gubbins, D. & Kelly, P. 1993 Persistent patterns in the geomagnetic field over the past 2.5 Ma. *Nature* **365**, 829–832.

Hulot, G., Le Mouel, J.-L. & Jault, D. 1990 The flow at the core–mantle boundary: symmetry properties. *J. Geomag. Geoelectr.* **42**, 857–874.

Loper, D. E. 1990 Dynamo energetics and the structure of the outer core. *Geophys. Astrophys. Fluid Dyn.* **49**, 231.

McFadden, P. L., Barton, C. E. & Merrill, R. T. 1993 Do virtual geomagnetic poles follow preferred paths during reversals? *Nature* **361**, 342–344.

Merrill, R. T. & McElhinny, M. W. 1983 *The Earth's magnetic field.* London: Academic.

Olson, P. & Glatzmaier, G. A. 1995 Magnetoconvection in a rotating spherical shell: structure of flow in the outer core. *Physics Earth Planet. Inter.* **92**, 109–118.

Prevot, M. & Camps, P. 1993 Absence of longitudinal confinement of poles in volcanic records of geomagnetic reversals. *Nature* **366**, 53–57.

Quidelleur, X., Valet, J.-P., Courtillot, V. & Hulot, G. 1994 Long-term geometry of the geomagnetic field for the last five million years: an updated secular variation database. *Geophys. Res. Lett.* **21**, 1639–1642.

Su, W.-J., Woodward, R. L. & Dziewonski, A. M. 1994 Degree-12 model of shear velocity heterogeneity in the mantle. *J. Geophys. Res.* **99**, 6945–6980.

Sun, Z.-P., Schubert, G. & Glatzmaier, G. A. 1994 Numerical simulations of thermal convection in a rapidly rotating spherical shell cooled inhomogeneously from above. *Geophys. Astrophys. Fluid Dyn.* **75**, 199–226.

Tackley, P. J., Stevenson, D. J., Glatzmaier, G. A. & Schubert, G. 1994 Effects of multiple phase transitions in a 3-D spherical model of convection in the earth's mantle. *J. Geophys. Res.* **99**, 15 877-15 901.

Tric, E., Laj, C., Jehanno, C., Valet, J.-P., Kissel, C., Mazaud, A. & Iaccarino, S. 1991 High resolution record of the upper olduvai transition from Po Valley (Italy) sediments: support for dipolar transition geometry? *Phys. Earth Planet. Inter.* **65**, 319–336.

Valet, J.-P., Tuchloka, P., Courtillot, V. & Meynadier, L. 1992 Paleomagnetic constraints on the geometry of the geomagnetic field during reversals. *Nature* **356**, 400–407.

Voorhies, C. V. 1993 Geomagnetic estimates of steady surficial core flow and flux diffusion: unexpected geodynamo experiments. In *Dynamics of Earth's deep interior and Earth rotation.* Geophysical monograph 72, IUGG vol. 12, pp. 113–125.

Zhang, K.-K. 1995 Spherical shell rotation convection in the presence of a toroidal magnetic field. *Proc. R. Soc. Lond.* A **448**, 245–268.

Zhang, K.-K. & Gubbins, D. 1993 Convection in a rotating spherical fluid shell with an inhomogeneous temperature boundary condition at infinite Prandtl number. *J. Fluid Mech.* **250**, 209–232.

Zhang, K.-K. & Jones, C. A. 1994 Convective motions in the Earth's fluid core. *Geophys. Res. Lett.* **21**, 1939–1942.

PHILOSOPHICAL TRANSACTIONS OF THE ROYAL SOCIETY A MATHEMATICAL, PHYSICAL & ENGINEERING SCIENCES